Carbohydrate Polymers 113 (2014) 539–551

Contents lists available at ScienceDirect

Carbohydrate Polymers

journal homepage: www.elsevier.com/locate/carbpol

Two-dimensional macromolecular distributions reveal detailed architectural features in high-amylose starches

Francisco Vilaplana[a,b,c], Di Meng[c], Jovin Hasjim[c], Robert G. Gilbert[a,c,*]

[a] Tongji School of Pharmacy, Huazhong University of Science and Technology, Wuhan 430030, Hubei, China
[b] KTH Royal Institute of Technology, Division of Glycoscience and Wallenberg Wood Science Centre (WWSC), AlbaNova University Centre, SE-106 91 Stockholm, Sweden
[c] The University of Queensland, Centre for Nutrition and Food Sciences, Queensland Alliance for Agriculture and Food Innovation, Brisbane 4072, QLD, Australia

ARTICLE INFO

Article history:
Received 21 March 2014
Received in revised form 13 July 2014
Accepted 15 July 2014
Available online 31 July 2014

Keywords:
Branching
Size-exclusion chromatography
Starch
Amylose
Amylopectin
Intermediate components

ABSTRACT

Two-dimensional (2D) structural distributions based on macromolecular size and branch chain-length are obtained for three maize starches with different amylose contents (one normal and two high-amylose varieties). Data were obtained using an analytical methodology combining chemical fractionation, enzymatic debranching, and offline 2D size-exclusion chromatography with multiple detection. The 2D distributions reveal novel features in the branching structure of high-amylose maize starches. Normal maize starch shows well-resolved structural topologies, corresponding to the amylopectin and amylose macromolecular populations. However, high-amylose maize starches exhibit very complex topologies with significant features between those of amylose and amylopectin, showing the presence of distinct intermediate components. These have the macromolecular size of amylose but similar branching structure to amylopectin, except for a higher proportion of longer branches. These structural features of the intermediate components can be related to a less tightly controlled biosynthesis of the branching structures in high-amylose maize starch mutants, which may prevent these molecules from maturing into full-size amylopectin. This altered macromolecular branched architecture of high-amylose starches probably contribute to their better nutritional properties.

1. Introduction

Starch is a complex branched homopolymer of glucose, whose polymeric chains are extended through α-(1 → 4) glycosidic linkages and branched by α-(1 → 6) glycosidic linkages. The structure of these molecules can be divided into multiple levels, of which the first two are as follows: Level 1, that of the individual chains (which provides the convenient categories of long- and short-chain branches) and Level 2, that of molecularly-disperse whole (branched) molecules.

Two main macromolecular populations with distinct architecture have been traditionally identified in starch: "almost-linear" amylose (AM) with a molecular weight between 10^4 and 10^6 and a few long-chain branches, and hyperbranched amylopectin (AP) composed of short glucose branches forming clusters that can reach molecular weights of 10^7–10^9. However, this division based on branching structure and molecular size is not clear-cut in some mutant starches, where additional macromolecular populations, such as intermediate components (IC), are present (Lansky, Kooi, & Schoch, 1949; Whistler & Doane, 1961). IC is defined as a macromolecular population with a similar branching structure to AP, but with the molecular size similar to AM (Baba & Arai, 1984; Kasemsuwan, Jane, Schnable, Stinard, & Robertson, 1995; Li, Jiang, Campbell, Blanco, & Jane, 2008). For example, high-amylose maize starches (HAMS), commercially obtained from plants with an amylose-extender (*ae*) mutant gene, possess substantial amounts of IC. In addition, they also contain more AM and a larger proportion of long AP branches than normal maize starches. High-amylose starches have been reported to have nutritional benefits because of their high amounts of resistant starch (RS), which is a portion of starch not digested by enzymes in the small intestine and an important substrate for gut microbial fermentation in the colon (Englyst, Kingman, & Cummings, 1992). This higher amount of RS in HAMS is believed to be related to their altered macromolecular

* Corresponding author at: The University of Queensland, Centre for Nutrition and Food Sciences, CNAFS, Building 83-S434, Brisbane 4072, QLD, Australia.
Tel.: +61 7 3365 4809; fax: +61 7 3365 1188.
E-mail address: b.gilbert@uq.edu.au (R.G. Gilbert).

http://dx.doi.org/10.1016/j.carbpol.2014.07.050
0144-8617/

architecture in terms of branching (Englyst et al., 1992; Htoon et al., 2009; Kasemsuwan et al., 1995; Li et al., 2008; Lopez-Rubio, Flanagan, Shrestha, Gidley, & Gilbert, 2008).

Advanced characterisation techniques to analyse the complex branching structure of starch molecules are useful to understand the properties and nutritional effects of starch. In a previous study (Vilaplana & Gilbert, 2010a, 2010b, 2011), we developed an integrated enzymatic and chromatographic protocol to obtain 2-dimensional (2D) structural distributions based on macromolecular size and branch chain-length of starch. In this method, starch molecules are fractionated in the first dimension based on their macromolecular size (e.g. hydrodynamic volume, V_h) using preparative size-exclusion chromatography (SEC), and subsequently debranched using isoamylase, a specific enzyme that quantitatively cleaves the α-(1 → 6) glycosidic linkages at the branching points. Each branch is released as a linear molecule, which is further characterised by analytical SEC to obtain the chain-length distribution (CLD) as the second dimension, and finally the results from both dimensions are mathematically combined to provide the 2D macromolecular distribution. These 2D distributions of molecular structure offer an extended view of their macromolecular architectures and reveal detailed structural features that can be linked to their biosynthetic processes and properties. Additionally, we have used these 2D distributions to validate the traditional *definitions* of AM and AP based on *characterisation* methods (e.g. colorimetric assays), where the results indicated that there is no rigorous definition of how a starch molecule can be classified unambiguously as AM or AP, especially in mutant starches where substantial amounts of hybrid or intermediate populations are present (Vilaplana, Hasjim, & Gilbert, 2012). Thus an improved comprehensive topological description of the branching structure and molecular size of the different molecular populations in starch can be obtained using 2D distributions rather than the conventional one-dimensional ones of Level 1 CLDs and Level 2 overall size distributions.

In this article, an integrated methodology combining chemical, enzymatic and chromatographic approaches is applied to explore the branching architectures of the molecular populations present in HAMS and normal maize starch (NMS). The resulting 2D macromolecular distributions are interpreted in terms of the underlying starch biosynthetic processes and properties, such as digestibility, related to the nutritional benefits of the starch. The present work complements previous studies on *ae* starches by Jiang, Campbell, Blanco, and Jane (2010) and Li et al. (2008).

2. Materials and methods

2.1. Materials

Three commercial maize starches with different AM contents were purchased from Penford Australia Ltd. (Lane Cove, NSW, Australia): one NMS and two HAMS (Gelose 50 or G50, and Gelose 80 or G80). Their AM contents range between 30 and 35%, 48 and 64%, and 58 and 83%, respectively, the reported value depending on the analytical techniques (Vilaplana et al., 2012).

2.2. Chemical fractionation of the starches

Parent (or unfractionated) starch samples (labelled NMS-ST, G50-ST, and G80-ST) were chemically fractionated with *n*-butanol to isolate their AM and AP populations, adapting established alcohol fractionation methodologies (e.g. Schoch, 1942; Lansky et al., 1949; Klucinec & Thompson, 1998). Each starch (1 g) was defatted prior to *n*-butanol fractionation by dissolving the starch in 100 mL dimethyl sulfoxide (DMSO) solution (90%, v/v) in a boiling water bath for 1 h, subsequent stirring at room temperature for an additional 16 h, and precipitation with five volumes of absolute ethanol. The precipitate was resuspended with 100 mL hot deionized water, and the pH was adjusted to 6 using a phosphate buffer. The starch suspension was refluxed in a boiling water bath for 1 h with stirring prior to the addition of 20 mL *n*-butanol and refluxing continued for an additional 30 min. The sample was then cooled slowly in an insulated box to room temperature for about 30 h prior to centrifugation. The precipitate contains mainly the AM component (labelled as NMS-AM, G50-AM, and G80-AM) with long linear chains that form helical complexes with *n*-butanol, whereas the supernatant constitutes mainly the AP component (labelled as NMS-AP, G50-AP, and G80-AP), whose branches are too short to form complexes with *n*-butanol. The short-branched component in the supernatant was further purified by repeating the *n*-butanol fractionation procedure twice and collected through precipitation with five volumes of absolute methanol. Both AM and AP components were washed with absolute ethanol prior to vacuum filtration and drying.

2.3. Size fractionation and debranching of starch

The 2D distributions of the parent (unfractionated) starch samples and the AP and AM fractions were obtained using a previous procedure combining 2D offline SEC and enzymatic debranching (Vilaplana & Gilbert, 2010a, 2010b, 2011). In brief, the unfractionated starch samples and their AM and AP fractions were dissolved in an SEC eluent, consisting of DMSO (ACS grade, Merck, Kilsyth, VIC, Australia) with 0.5% w/w LiBr (ReagentPlus, Sigma–Aldrich, Castle Hill, NSW, Australia) to a concentration of 10 g L^{-1} in a thermomixer (Eppendorf, Hamburg, Germany) set at 80 °C for 8 h with agitation at 350 rpm. Size fractionation was performed by preparative SEC using GRAM Precolumn, GRAM 30 and GRAM 3000 preparative columns, from Polymer Standards Service (PSS, Mainz, Germany) thermostated at 80 °C. The preparative SEC set-up was calibrated by the injection of pullulan standards (see Section 2.4 for further details), which allowed the calculation of the preparative SEC weight distributions, $w(\log V_h)_{PREP}$. Each starch size fraction was collected manually at different elution volumes, precipitated using five volumes of absolute ethanol, and centrifuged at 4000 × *g*. The starch in each size fraction was debranched using isoamylase from *Pseudomonas* sp. (Megazyme International Ltd., Bray, Co. Wicklow, Ireland) following a method described elsewhere (Hasjim, Cesbron-Lavau, Gidley, & Gilbert, 2010), and freeze-dried prior to redissolution in the SEC eluent.

2.4. Offline analytical size-exclusion chromatography

The different fractions after chemical fractionation with *n*-butanol and after size fractionation by preparative SEC, both in their native (branched) state and debranched state after isoamylase treatment, were characterised using analytical SEC (Agilent 1100 equipment, Agilent Technologies, Waldbronn, Germany), following a previous procedure, with minimal shear scission of the AP fraction in the "branched" set-up and enhanced separation in the "debranched" set-up (Cave, Seabrook, Gidley, & Gilbert, 2009). Detection was carried out using a multiple-angle laser light scattering detector (MALLS, BIC-MwA7000, Brookhaven Instrument Corp., Holtsville, NY, USA), and a refractive index detector (RID-10A, Shimadzu, Kyoto, Japan) thermostatted at 45 °C. The separation of the branched samples was carried out using combined GRAM Precolumn, GRAM 30, and GRAM 3000 analytical columns (PSS, Mainz, Germany) with DMSO containing 0.5% w/w LiBr at 80 °C and at a flow rate of 0.3 mL min^{-1}, and the analysis of the debranched samples was performed with combined GRAM Precolumn, GRAM 10, and GRAM 1000 analytical columns (PSS) with DMSO containing 0.5% w/w LiBr at 80 °C and at a flow

rate of 0.6 mL min^{-1}. Mark–Houwink calibration was performed by injection of pullulan standards (PSS). The Mark–Houwink parameters for pullulan in DMSO with 0.5% w/w LiBr at 80 °C are $K = 2.427 \times 10^{-4}$ dL g^{-1} and $a = 0.6804$ (Kramer and Kilz, PSS, Mainz, Germany, private communication). The data recorded from the analytical SEC separations and multiple detection were analysed using WinGPC software (PSS) and further processed to obtain the SEC weight distribution $w(\log V_h)$, the branch chain-length distributions $w(\log X_{de})$ and $N(X_{de})$, the size dependence of the weight-average molecular weight $M_w(V_h)$, and the 2D macromolecular size/branch chain-length distributions $w(\log(V_h, X_{de}))$ (Gaborieau, Gilbert, Gray-Weale, Hernandez, & Castignolles, 2007; Vilaplana & Gilbert, 2010a, 2010b). The macromolecular size distributions of branched samples are presented against hydrodynamic radius (R_h), with $V_h = 4/3\pi R_h^3$ obtained from Mark–Houwink calibration of the elution volumes, and their branch chain-length distributions from debranched samples are presented against average degree of polymerisation (DP) (X_{de}, where the subscript "de" indicates debranched starch) from light scattering calibration.

3. Results and discussion

3.1. Chemical fractionation of maize starches

Fractionation of starch using *n*-butanol is expected to generate two macromolecular fractions with different branch chain-lengths: the precipitated populations with long linear branches that are mainly attributed to AM and the populations with short branches in the supernatant that mainly originated from AP (Lansky et al., 1949; Whistler & Doane, 1961). Fig. 1 shows the SEC weight distributions $w(\log V_h)$ (which is the same as $w(\log R_h)$ within an arbitrary constant) and the size dependence of weight-average molecular weight distributions $M_w(R_h)$ of the three parent starch samples (NMS-ST, G50-ST, and G80-ST) and their AM and AP fractions obtained from *n*-butanol precipitation. The distributions for NMS show that *n*-butanol can effectively precipitate the AM component of M_w around 10^6 with minor AP contaminations of larger M_w (around 10^8), and most AP molecules remain in the supernatant. The separation of the AM fractions through *n*-butanol precipitation is also successful for the HAMS varieties (G50 and G80). Interestingly, the $w(\log V_h)$ distributions of the AP fractions in the HAMS varieties show very heterogeneous distributions of branched populations throughout a wide range of macromolecular size, which can be assigned to the AP and IC populations. The hydrodynamic sizes of AP fractions from HAMS, however, are smaller than expected. These anomalous results might have been caused by molecular degradation and/or incomplete redissolution after *n*-butanol fractionation prior to injection into the analytical SEC set-up. The recoveries of the starch molecules after SEC separation were measured for the parent samples (NMS-ST, G50-ST, and G80-ST) and their AM and AP fractions. The ST and AM fractions for all three starch materials and the AP fraction from NMS (NMS-AP) offered quantitative recovery (>95%), whereas the AP fractions from the HAMS (G50-AP and G80-AP) showed a lower recovery (around 60%). The lower recovery is an indication of the degradation and/or the incomplete redissolution of the AP fractions from HAMS. However, this does not affect the branch chain-length distributions and the constructed 2D distributions of HAMS. The debranched samples have smaller molecules than their branched counterparts, increasing their solubility and facilitating the redissolution. Furthermore, although cleaving one or two inner branches of a starch molecule can greatly reduce its molecular size (such as by half and third, respectively, if the new molecules are about the same size), the amount of intact branches is far more than that of cleaved branches, leaving no apparent changes in the branch chain-length distribution.

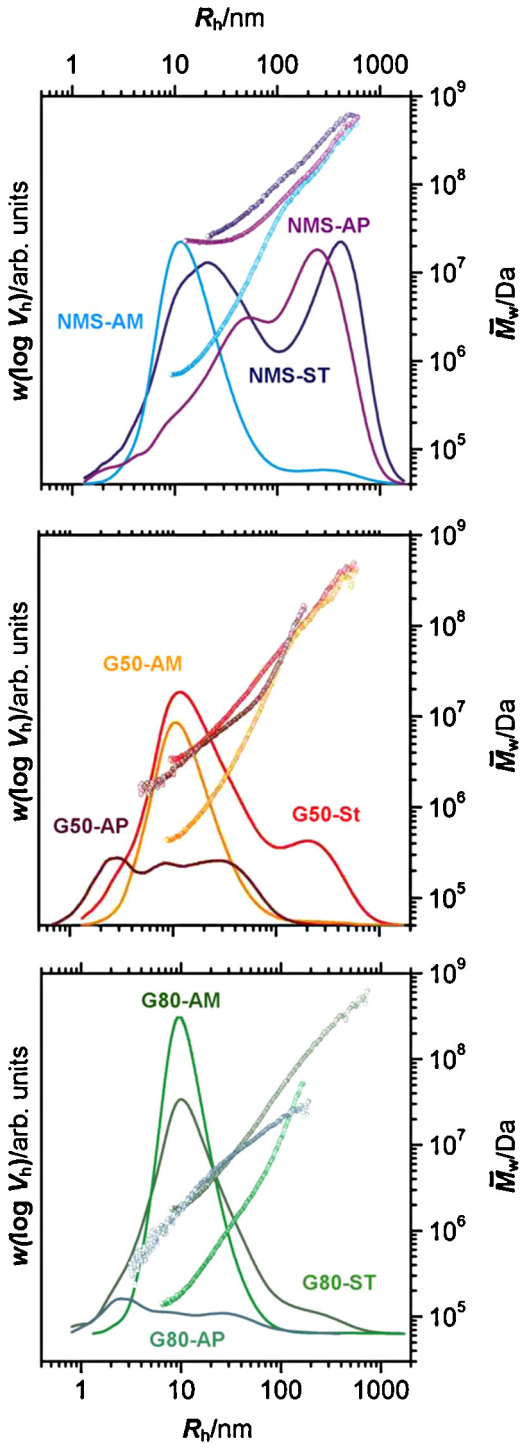

Fig. 1. SEC weight [$w(\log V_h)$] and weight-average molecular weight [$M_w(V_h)$] distributions of parent (or unfractionated) maize starches and their fractions after chemical fractionation using *n*-butanol, as functions of hydrodynamic radius.

Fig. 2 shows the number $N(X_{de})$ and weight $w(\log X_{de})$ chain-length distributions of the parent starches (NMS-ST, G50-ST, and G80-ST), and of their AM and AP fractions from *n*-butanol precipitation treatment. In general, the chain-length distributions of all samples exhibit the characteristic multimodal pattern of debranched starch. The AP branches (between $X_{de} \sim 5$ and 100) from all samples show a bimodal distribution of single-lamellar branches (AP1, between $X_{de} \sim 5$ and 35) and lamella-spanning branches (AP2, between $X_{de} \sim 35$ and 100), whereas the AM

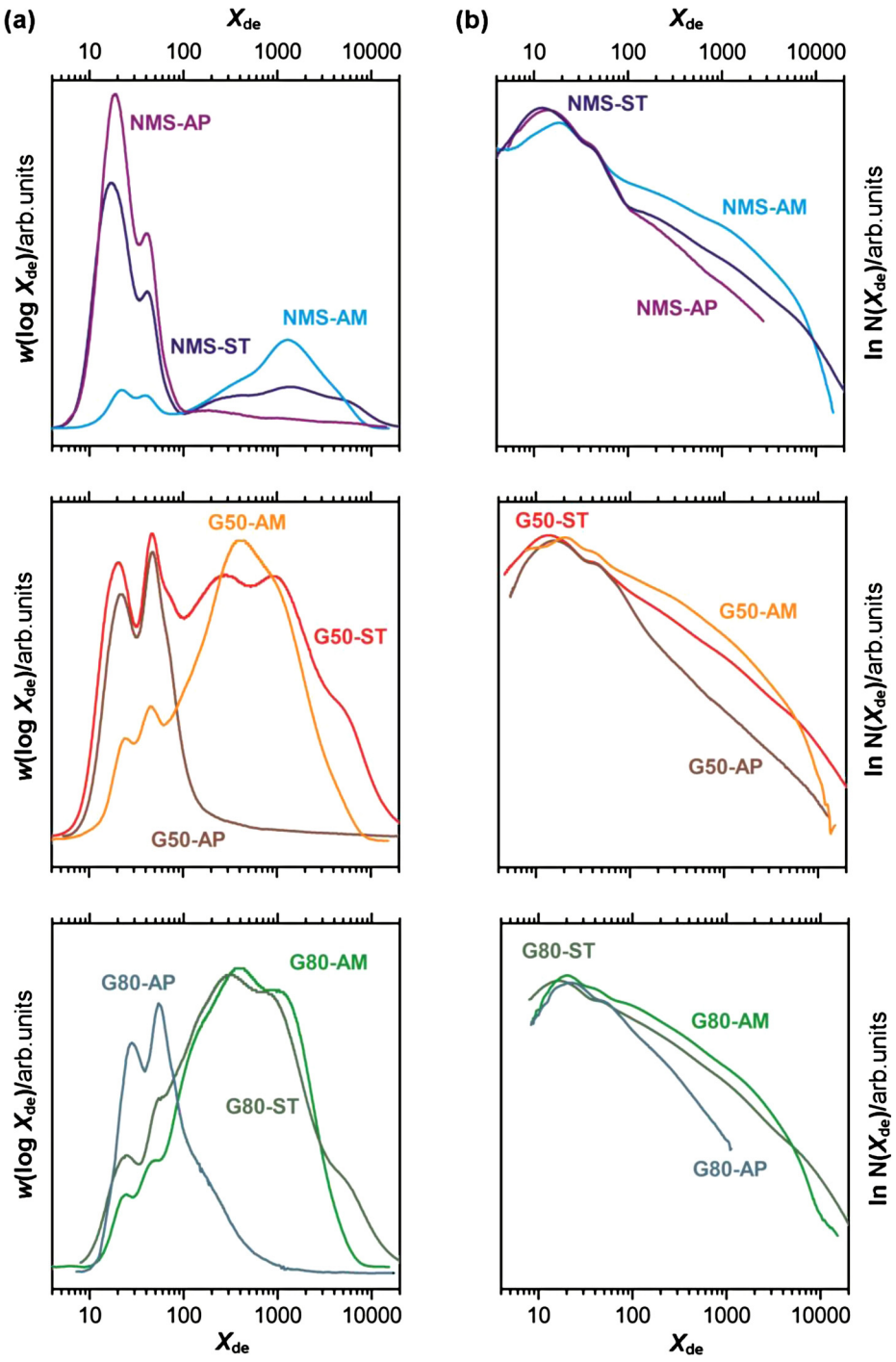

Fig. 2. Branch chain-length distributions of parent (or unfractionated) maize starches and their fractions after chemical fractionation using *n*-butanol precipitation, as functions of average degree of polymerisation X_{de}: (a) weight $w(\log X_{de})$ and (b) number $N(X_{de})$ distributions.

branches (between $X_{de} \sim 100$ and 20,000) from the parent starch samples and their AM fractions show a multimodal curve. The AP fractions contain mainly short-branched populations, attributed to AP and IC. The efficiency of the *n*-butanol fractionation in separating the macromolecular populations with short branches from those with long linear branches is verified from these chain-length distributions. Interestingly, all AM fractions contain traces of short branches, which may arise from AP impurities and/or from the presence of short branches in AM as "immature clusters" (Takeda, Shitaozono, & Hizukuri, 1990). These assignments will be further examined below from the 2D distributions obtained from size fractionation using preparative SEC. All parent starch samples (NMS-St, G50-St, and G80-St) also exhibit a shoulder for large chain length ($X_{de} > 5000$) that is somewhat reduced in the precipitated fractions after *n*-butanol treatment (NMS-AM, G50-AM, G80-AM). This could be caused by either partial degradation of the larger AM branches during *n*-butanol treatment or incomplete DMSO/LiBr redissolution after the fractionation and ethanol precipitation. This result highlights again the harsh nature of the chemical fractionation treatment on the larger starch molecules. The effect of *n*-butanol

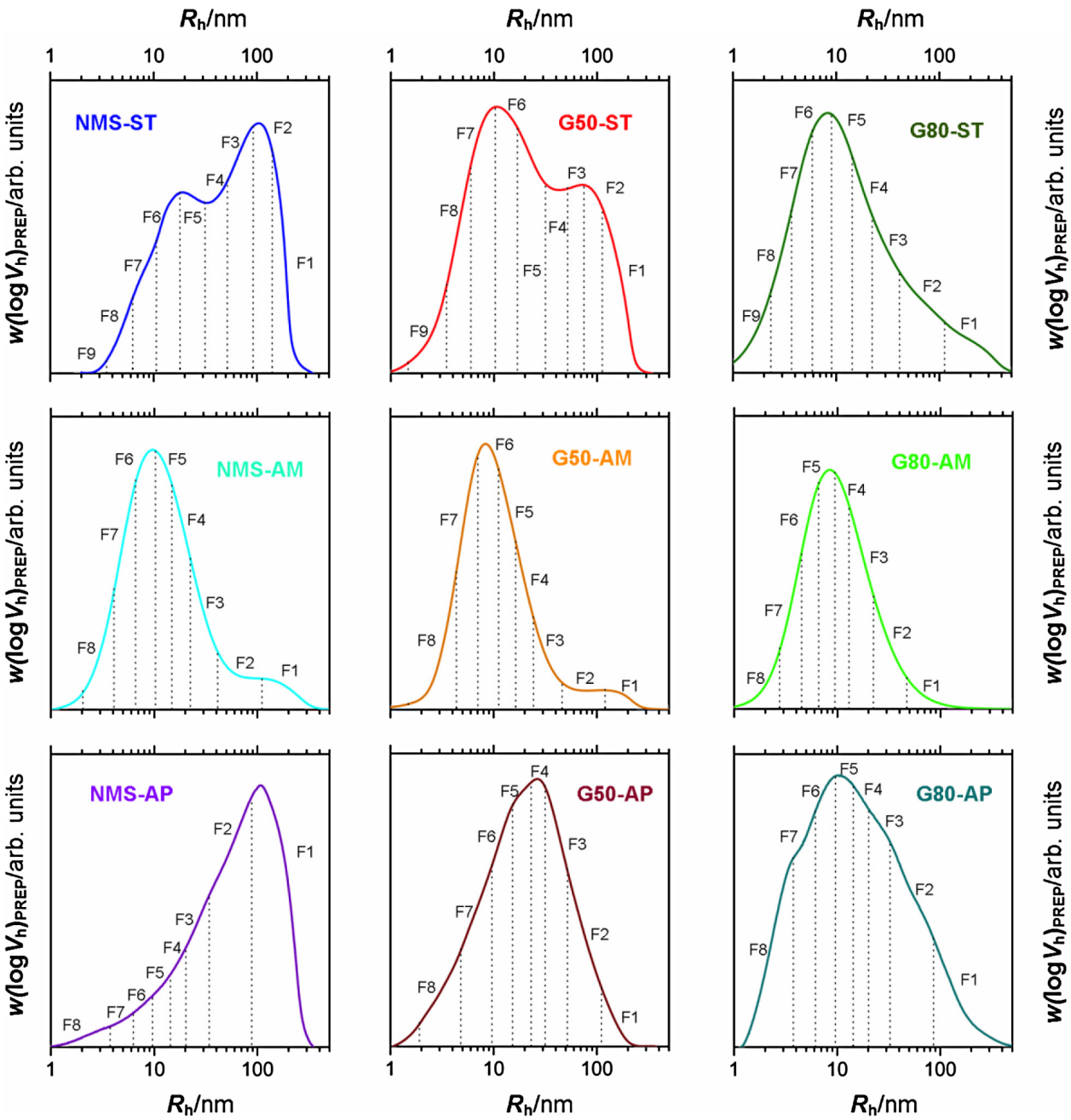

Fig. 3. SEC weight distributions [$w(\log V_h)$] using preparative SEC and fraction collection intervals of the different parent maize starches as well as their AM and AP fractions. The broken vertical lines delimit the collected fractions in correspondence with the conditions in Supplementary information Table S1.

fractionation on the macromolecular architectures of both AM and AP constitutes an interesting study that should be conducted separately in detail.

3.2. Size fractionation of maize starches and construction of two-dimensional distributions

Size fractionation of the parent starch samples (NMS-ST, G50-ST, and G80-ST) and their AM and AP fractions from *n*-butanol precipitation was performed using preparative SEC. The preparative SEC weight distributions $w(\log V_h)_{PREP}$ and the fraction collection intervals are shown in Fig. 3 and Supplementary information Table S1. The preparative SEC weight distributions match their corresponding analytical SEC weight distributions in Fig. 1, confirming that the procedure was successful and therefore suitable to obtain the 2D macromolecular size/chain-length distributions for different parent starches and their AM and AP fractions. Each size fraction was debranched using isoamylase and then characterised using analytical SEC to obtain their branch chain-length distributions (Fig. 4). Structural parameters extracted from the branch chain-length distributions were the number- and weight-average DPs ($X_{de,n}$ and $X_{de,w}$, respectively) for each branch population (AP1, AP2, and AM branches), and the peak height ratio of the longer to the shorter AP branches (AP2/AP1). These results for NMS, G50, and G80 are shown in Tables 1–3, respectively.

3.3. Two-dimensional distributions for normal maize starch

The chain-length distribution of debranched NMS-ST exhibits clearly separated zones of AP and AM branches (Fig. 4). The

Table 1
Structural features of normal maize starch fractions collected from size fractionation.

Sample	$\bar{R}_h$ (nm)	AP1 branches ($X_{de} \sim 5$–35)		AP2 branches ($X_{de} \sim 35$–100)		Height ratio	AM branches ($X_{de} \sim 100$–20,000)	
		$\bar{X}_{de,n}$	$\bar{X}_{de,w}$	$\bar{X}_{de,n}$	$\bar{X}_{de,w}$	AP2/AP1	$\bar{X}_{de,n}$	$\bar{X}_{de,w}$
Parent or unfractionated starch (NMS-ST)								
Whole	–	16	17	47	48	0.56	905	1134
*F*1	224	17	18	45	46	0.54	–	–
*F*2	115	16	17	48	48	0.55	–	–
*F*3	69	17	17	47	46	0.52	2597	2758
*F*4	41	16	17	48	48	0.58	2257	2418
*F*5	23	17	18	48	48	0.54	2259	2485
*F*6	14	17	18	53	54	0.69	1604	1712
*F*7	8	17	18	48	51	0.61	765	836
*F*8	5	17	18	49	50	0.61	302	338
*F*9	3	20	20	–	–	–	162	179
Amylose fraction (NMS-AM)								
Whole	–	17	18	46	47	0.85	850	969
*F*1	214	17	18	47	48	0.56	–	–
*F*2	69	17	18	48	49	0.56	1710	1872
*F*3	30	16	17	49	49	0.56	3048	3272
*F*4	18	17	18	53	54	0.72	2097	2242
*F*5	12	18	19	54	55	0.77	1327	1468
*F*6	8	17	18	58	59	1.25	736	827
*F*7	5	18	19	–	–	–	320	435
*F*8	3	–	–	–	–	–	144	160
Amylopectin fraction (NMS-AP)								
Whole	–	17	18	47	48	0.58	1818	1982
*F*1	186	16	16	46	47	0.54	–	–
*F*2	54	16	17	48	49	0.57	–	–
*F*3	26	16	17	46	47	0.56	2512	2592
*F*4	17	17	18	47	48	0.57	1924	2159
*F*5	12	16	16	48	56	0.59	1145	1146
*F*6	8	17	18	51	53	0.67	–	–
*F*7	5	17	18	52	53	0.68	–	–
*F*8	2	18	19	49	50	1.00	–	–

Table 2
Structural features of Gelose 50 starch fractions collected from size fractionation.

Sample	R_h (nm)	AP1 branches ($X_{de} \sim 5$–35)		AP2 branches ($X_{de} \sim 35$–100)		Height ratio	AM branches ($X_{de} \sim 100$–20,000)	
		$X_{de,n}$	$X_{de,w}$	$X_{de,n}$	$X_{de,w}$	AP2/AP1	$X_{de,n}$	$X_{de,w}$
Parent or unfractionated starch (G50-ST)								
Whole	–	17	18	55	57	1.11	629	797
*F*1	204	19	19	55	56	1.03	–	–
*F*2	93	18	19	54	56	1.04	–	–
*F*3	63	18	19	54	56	1.10	–	–
*F*4	41	18	19	56	58	1.12	5080	5128
*F*5	23	19	19	56	58	1.14	2350	2598
*F*6	13	19	19	58	60	1.23	1100	1190
*F*7	8	19	19	59	61	1.28	666	722
*F*8	5	19	20	54	55	1.51	295	323
*F*9	2	–	–	–	–	–	68	83
Amylose fraction (G50-AM)								
Whole	–	19	20	44	45	1.31	423	508
*F*1	229	20	20	53	55	1.05	–	–
*F*2	76	18	19	54	55	1.03	3354	3613
*F*3	34	17	18	55	56	1.18	3089	3308
*F*4	20	18	19	55	57	1.15	2325	2330
*F*5	13	20	20	57	58	1.42	1206	1332
*F*6	9	18	19	58	59	–	680	738
*F*7	6	–	–	–	–	–	304	337
*F*8	3	–	–	–	–	–	109	167
Amylopectin fraction (G50-AP)								
Whole	–	19	20	55	57	1.18	1440	1781
*F*1	204	19	19	53	54	0.94	–	–
*F*2	78	18	19	55	56	1.04	–	–
*F*3	41	18	19	56	56	1.08	–	–
*F*4	28	18	19	56	57	1.10	1955	2041
*F*5	19	18	19	55	57	1.09	1345	1411
*F*6	12	18	19	59	61	1.13	636	688
*F*7	7	18	19	59	61	1.18	447	483
*F*8	3	18	19	55	57	1.51	256	269

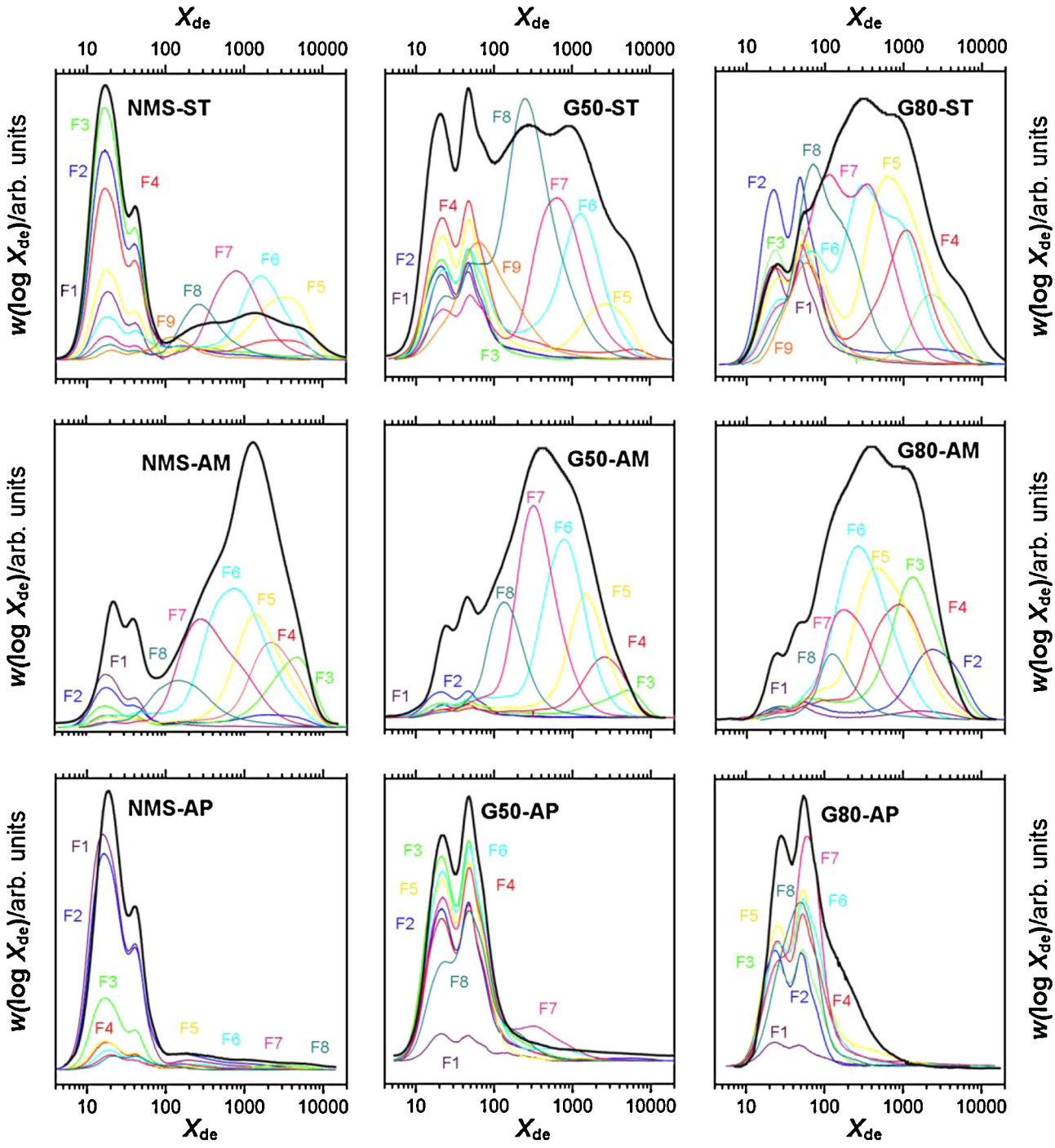

Fig. 4. SEC weight chain-length distributions [$w(\log X_{de})$] after preparative SEC size fractionation (corresponding to Fig. 3) and isoamylase debranching of the parent maize starches and of their AM and AP fractions. The samples without preparative SEC size fractionation are displayed by black lines; coloured distributions are the collected size fractions. The distributions of the size fractions fall well under the umbrella of their respective sample without size fractionation. (For interpretation of the references to colour in this figure legend, the reader is referred to the web version of this article.)

starch fractions with larger macromolecular sizes (*F*1–*F*4, branched $R_h \sim 40$–225 nm, Table 1) are mainly composed of short (AP-type) branches. For Fractions *F*2–*F*4, branches of DP $X_{de} \sim 200$–300 are observed, which may belong to AP populations with extra-long chain branches, as it has been previously reported for starches from different botanical sources (Hanashiro, Matsugasako, Egashira, & Takeda, 2005). These extra-long chain branches are not noticeable in the chain-length distribution of the parent NMS-ST sample prior to size fractionation because they are masked by AM branches. The peak height ratio (AP2/AP1) is relatively constant from Fractions *F*1 to *F*5, with an average of 0.55, and slightly increases for *F*6–*F*8 (Table 1), indicating a larger proportion of longer lamellae-spanning AP branches for fractions with lower macromolecular sizes. This fact could be ascribed to the presence of IC (Baba & Arai, 1984; Kasemsuwan et al., 1995; Li et al., 2008) – macromolecules with a branching structure similar to AP, but with the macromolecular size similar to AM – as discussed later in detail. AM branches appear from Fractions *F*4 to *F*9 (branched $R_h \sim 3$–40 nm, Table 1),

Table 3
Structural features of Gelose 80 starch fractions collected from size fractionation.

Sample	R_h (nm)	AP1 branches (X_{de} ~5–35)		AP2 branches (X_{de} ~35–100)		Height ratio	AM branches X_{de} ~100–20,000)	
		$X_{de,n}$	$X_{de,w}$	$X_{de,n}$	$X_{de,w}$	AP2/AP1	$X_{de,n}$	$X_{de,w}$
Parent or unfractionated starch (G80-ST)								
Whole	–	20	21	–	–	–	548	609
*F*1	302	19	20	56	58	1.06		
*F*2	69	19	20	57	58	1.07	1985	2159
*F*3	30	19	20	58	60	1.18	2259	2380
*F*4	18	20	21	59	61	1.24	907	979
*F*5	11	20	21	63	65	1.43	796	875
*F*6	7	20	21	64	66	1.73	470	523
*F*7	5	21	22	84	88	3.05	422	448
*F*8	3	23	23	59	66	–	260	232
*F*9	1	–	–	–	–	–	62	72
Amylose fraction (G80-AM)								
Whole	–	20	21	42	43	–	400	406
*F*1	148	23	23	60	62	1.20	1239	1425
*F*2	32	21	22	65	67	1.32	2216	2325
*F*3	17	23	23	65	78	1.68	1194	1294
*F*4	11	21	22	76	78	2.42	816	899
*F*5	8	23	23	–	–	–	545	604
*F*6	5	–	–	–	–	–	246	288
*F*7	4	–	–	–	–	–	166	200
*F*8	2	–	–	–	–	–	141	161
Amylopectin fraction (G80-AP)								
Whole	–	22	26	60	61	1.20	–	–
*F*1	186	20	23	59	60	0.89	–	–
*F*2	54	21	24	57	58	0.98	–	–
*F*3	26	21	25	60	62	1.15	2252	2462
*F*4	17	22	26	62	64	1.21	1526	1684
*F*5	12	21	25	62	64	1.25	537	634
*F*6	8	22	26	63	65	1.36	–	–
*F*7	5	21	29	61	63	2.15	–	–
*F*8	2	–	–	40	44	–	–	–

and the main peak of the chain-length distributions shifts to lower DP (shorter AM branches) with decreasing branched macromolecular size. This observation has also been reported for normal rice starch (Vilaplana & Gilbert, 2010b).

The NMS-AM sample shows that long (AM-type) branches are clearly distinguished in the chain-length distributions (Fig. 4), exhibiting a multimodal shape that could originate from different biosynthetic pathways of AM in the maize kernel, such as involvement of starch branching enzymes (SBE) or different isoforms of granule-bound starch synthase (GBSS). Fractions with larger macromolecular sizes, such as Fractions *F*1 and *F*2 (branched R_h ~70–215 nm, Table 1), also show short (AP-type) branches. These short branches may be AP contaminations in the NMS-AM fraction obtained from the *n*-butanol precipitation treatment, which can be clearly observed in the SEC weight distribution of the branched sample from NMS-AM fraction (Fig. 1). However, traces of short branches in the range of the DP of AP branches can be found in every NMS-AM size fraction, indicating the presence of IC traces in these fractions and/or AM populations with a small number of short (AP-type) branches that have been reported as "immature clusters" (Takeda et al., 1990).

The NMS-AP fraction from the *n*-butanol chemical fractionation consists mainly of short (AP-type) branches (Fig. 4). The presence of AP with extra-long chain branches (between X_{de} ~200 and 300) can be observed, especially in Fractions *F*1 and *F*2 (branched R_h ~50–185 nm, Table 1), similar to that observed from Fractions *F*2–*F*4 of NMS-ST. Long AM-type branches are not observed in any size fractions of NMS-AP sample. All size fractions of NMS-AP sample have similar average DP $X_{de,n}$ and $X_{de,w}$ for both single-lamellae (AP1) and lamellae-spanning (AP2) branches regardless of the branched macromolecular size (Table 1), suggesting that the two distinct populations of AP branches are important for starch granular structure and the formation of semicrystalline lamellae. However, the AP2/AP1 ratio shows interesting behaviour similar to NMS-ST, as mentioned above. The AP2/AP1 ratio remains practically constant at a value of 0.55 from Fractions *F*1 to *F*4 (branched R_h ~20–185 nm, Table 1) and progressively increases for the fractions with smaller macromolecular sizes (branched R_h ~2–20 nm), which might have originated from IC, instead of AP.

The 2D macromolecular size/chain-length distributions of the NMS samples (NMS-ST, NMS-AM, and NMS-AP) are presented in Fig. 5. A clear separation between the two topological "mountains" assigned to AP and AM macromolecular populations can be observed as the result of both chemical and size fractionation in the 2D distributions. Small "foothills" can also be observed in the 2D distributions, corresponding to the minor populations of AP with extra-long chain branches and IC, but their presence is minor compared to the major components. These 2D distributions are similar to that obtained from normal rice starch in our previous paper (Vilaplana & Gilbert, 2010b), where a clear topological distinction between the AP and AM populations could be clearly observed, together with small "foothills" corresponding to AP with extra-long chain branches and IC. This indicates that normal starch varieties have topological distributions with distinct AM and AP populations, and trace amounts of hybrid components.

3.4. Two-dimensional distributions for high-amylose starches

The chain-length distributions of parent (or unfractionated) HAMS (G50-ST and G80-ST) prior to chemical fractionation exhibit a multimodal shape with no clear separation between the short (AP-type) branches and the long (AM-type) branches (Fig. 4), different from what was observed for NMS-ST. This indicates that HAMS contain larger amounts of IC species, as has been widely reported (e.g. Jane et al., 1999; Li et al., 2008). The size fractions with larger macromolecular sizes (Fractions *F*1–*F*3 for G50-ST and Fractions *F*1–*F*2 for G80-ST; branched R_h ~65–300 nm, Tables 2 and 3, respectively) are composed mainly of short branches, similar to those of

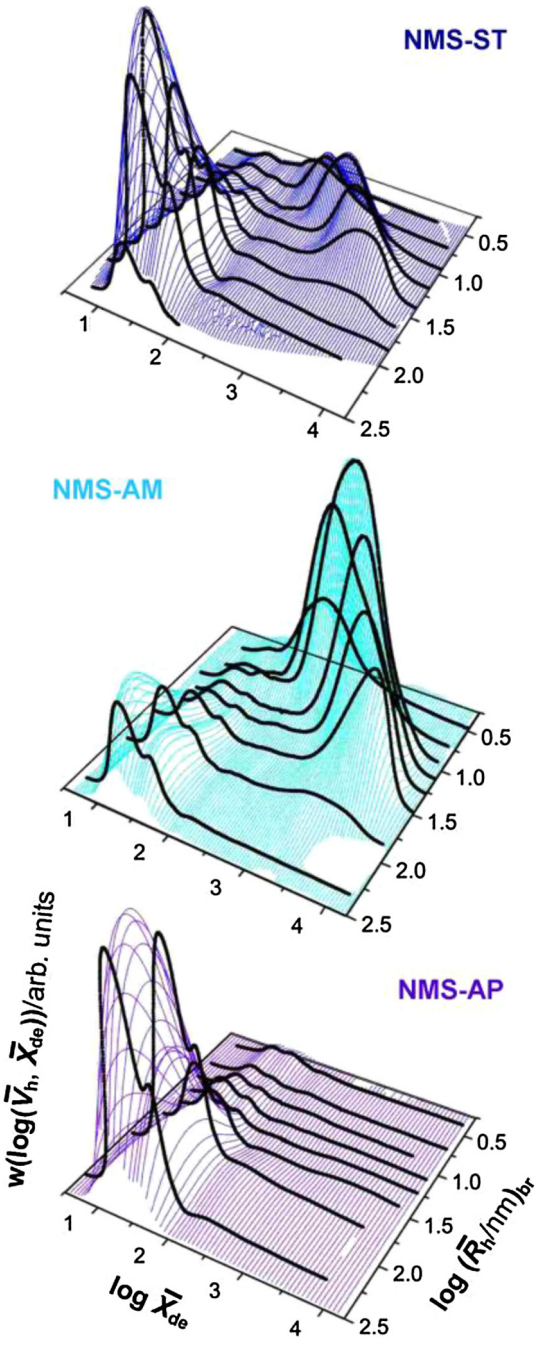

Fig. 5. Two-dimensional SEC weight distributions [$w(\log(R_h, X_{de}))$] of normal maize starch based on macromolecular size and branch chain-length. The black lines correspond to the experimental data from each collected size fraction obtained using preparative SEC. The coloured surface is obtained by Renka–Cline random gridding. A clear separation between the AP and the AM "mountains" can be observed in the surface plots, together with the small "foothills" corresponding to the IC and AP with extra-long chain branches. (For interpretation of the references to colour in this figure legend, the reader is referred to the web version of this article.)

NMS-ST, that are assigned to AP populations and can be divided into two peaks, i.e. single-lamella AP1 and lamellae-spanning AP2 branches. The amounts of these short branches are substantial in all size fractions, where the positions (or DP ranges) of AP1 and AP2 peaks are similar regardless of macromolecular sizes although the AP2/AP1 ratio changes. The average DPs of AP1 and AP2 of HAMS are higher than those of NMS, with G80 exhibiting the highest average DP ($X_{de,n} \sim 20$ and $X_{de,n} \sim 59$ for AP1 and AP2, respectively). Moreover, the AP2/AP1 ratios of HAMS are about double from those of NMS, showing that AP populations in HAMS contain larger proportions of lamellae-spanning AP branches than that in NMS, which can be related to their biosynthesis, as discussed below.

Long (AM-type) branches appear in larger proportions in HAMS fractions than in NMS fractions (Fig. 4). They are mainly present in the size fractions of G50-ST and G80-ST with smaller macromolecular sizes (branched $R_h \sim 3$–40 nm, Tables 2 and 3, respectively) and all size fractions of G50-AM and G80-AM. The main peak of the chain-length distributions shifts to lower DP (shorter AM branches) with decreasing branched macromolecular size, similar to that observed from NMS and that previously reported for normal rice starch (Vilaplana & Gilbert, 2010b). Traces of short (AP-type) branches can be found in every size fraction from the material precipitated by *n*-butanol, indicating again the presence of AP traces in the size fractions with larger macromolecular sizes (such as Fraction *F*2 of G50-AM), the presence of IC traces in the size fractions with smaller macromolecular sizes, and/or the presence of "immature clusters" in all size fractions of G50-AM and G80-AM.

A remarkable feature in the chain-length distributions of HAMS is the substantial amount of IC starting from Fractions *F*4 of G50-ST, G80-ST, G50-AP, and G80-AP (Fig. 4), with branched $R_h \sim 1$–40 nm (Tables 2 and 3 for G50 and G80, respectively). These IC are characterised by having similar average DP of the single-lamella branches (AP1) to AP components found in fractions with larger macromolecular sizes, but larger average DP of lamella-spanning branches (AP2) and higher AP2/AP1 ratio than AP. This feature could be used to distinguish between the branching structure of AP and IC.

This complex and heterogeneous branching architecture of the different macromolecular populations present in HAMS is clearly seen in the 2D distributions for G50-ST and G80-ST (Figs. 6 and 7, respectively), with no clear separation between the AP and AM "mountains" and a broad "intervalley" region attributed to IC. However, the chemical fractionation with *n*-butanol allows the independent analysis of the AM topologies in the G50-AM and G80-AM fractions separated from the IC and the identification of the topological features of both AP and IC in the G50-AP and G80-AP fractions. No clear topological separation can be observed in either 2D plots from ST and AP fractions for both branched components in HAMS, indicating a continuum of all macromolecular populations in HAMS.

3.5. Macromolecular populations in maize starches

The different macromolecular populations in maize starches are shown in Fig. 8 and are now discussed based on the 2D distributions,. which "tease apart" features such as longer amylopectin chains hidden under an amylose CLD.

3.5.1. Amylopectin

AP is the main macromolecular component in NMS and it is present in smaller amounts in HAMS mutants. Its typical bimodal distribution of short branches, consisting of single-lamellae and lamellae-spanning branches with constant average DP $X_{de,n}$ and $X_{de,w}$, is preserved throughout macromolecular sizes (Tables 1–3), excluding the fractions containing IC. This behaviour has been reported previously from 2D distribution of normal rice starch and discussed in terms of biosynthetic control of the chain distribution of AP branches throughout its macromolecular sizes, preserving the semicrystalline cluster organisation necessary for the formation of starch granules and for the survival of the grain (Vilaplana & Gilbert, 2010a, 2010b; Wu & Gilbert, 2010; Wu, Morell, & Gilbert, 2013; Wu, Ral, Morell, & Gilbert, 2014). The AP2/AP1 value is also preserved throughout all macromolecules sizes, although it is different between NMS and HAMS, indicating that the

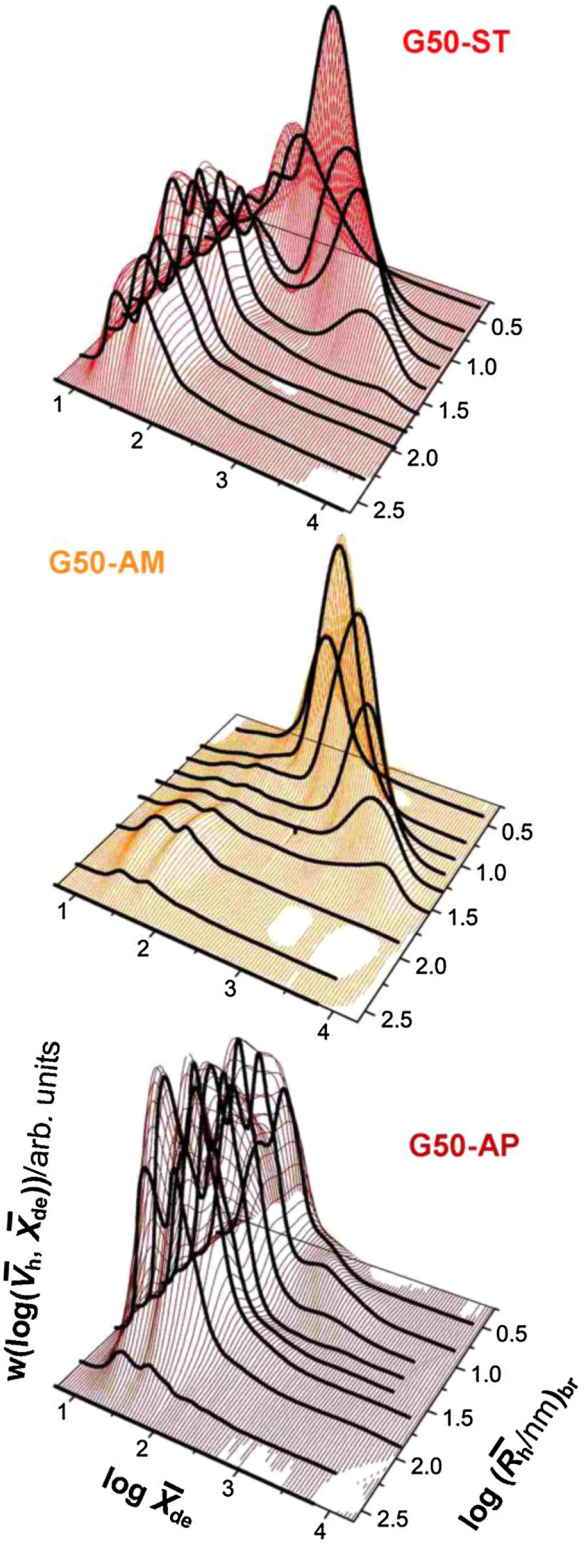

Fig. 6. Two-dimensional SEC weight distributions [$w(\log(R_h, X_{de}))$] of G50 starch based on macromolecular size and branch chain-length. The black lines correspond to the experimental data from each collected size fraction obtained using preparative SEC. The coloured surface corresponds to the mathematical distributions after Renka–Cline random gridding. (For interpretation of the references to colour in this figure legend, the reader is referred to the web version of this article.)

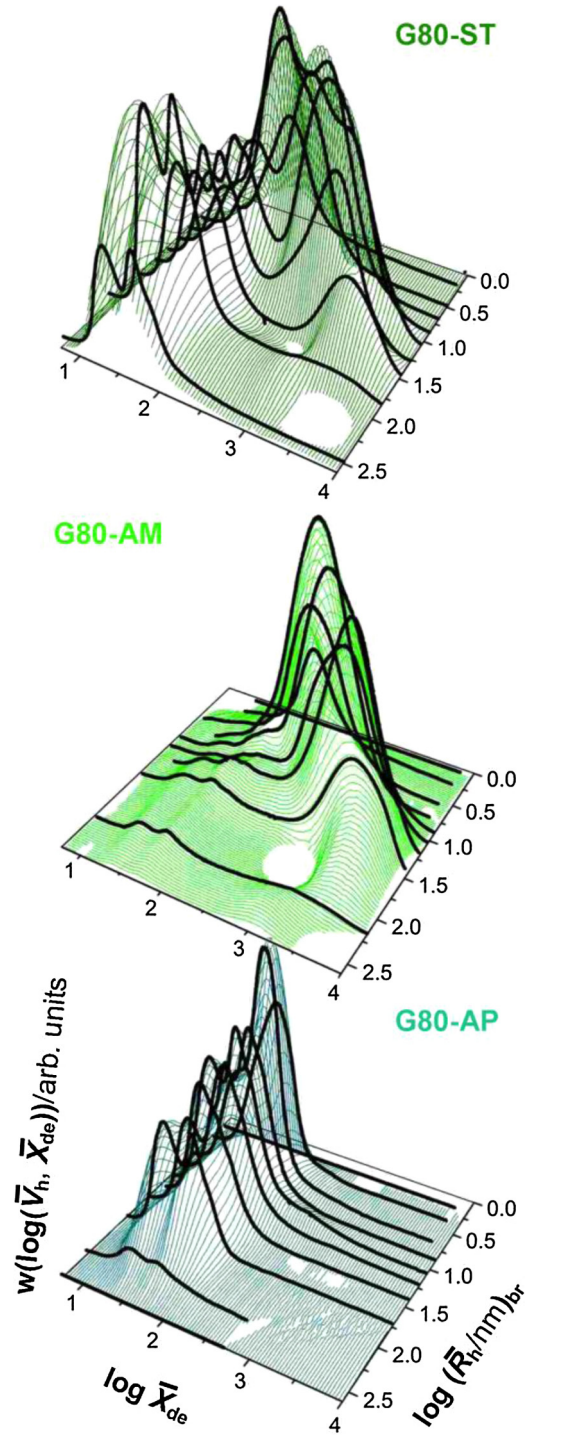

Fig. 7. Two-dimensional SEC weight distributions [$w(\log(R_h, X_{de}))$] for G80 starch based on macromolecular size and branch chain-length. The black lines correspond to the experimental data from each collected size fraction obtained using preparative SEC. The coloured surface corresponds to the mathematical distributions after Renka–Cline random gridding. (For interpretation of the references to colour in this figure legend, the reader is referred to the web version of this article.)

macromolecular structure of AP is tightly controlled by starch biosynthetic enzymes.

3.5.2. *Amylopectin with extra-long chain branches*

These extra-long chain branches of AP have been reported to be elongated by GBSS enzyme, which is the enzyme responsible for the synthesis of AM (Hanashiro et al., 2008). It is also possible that

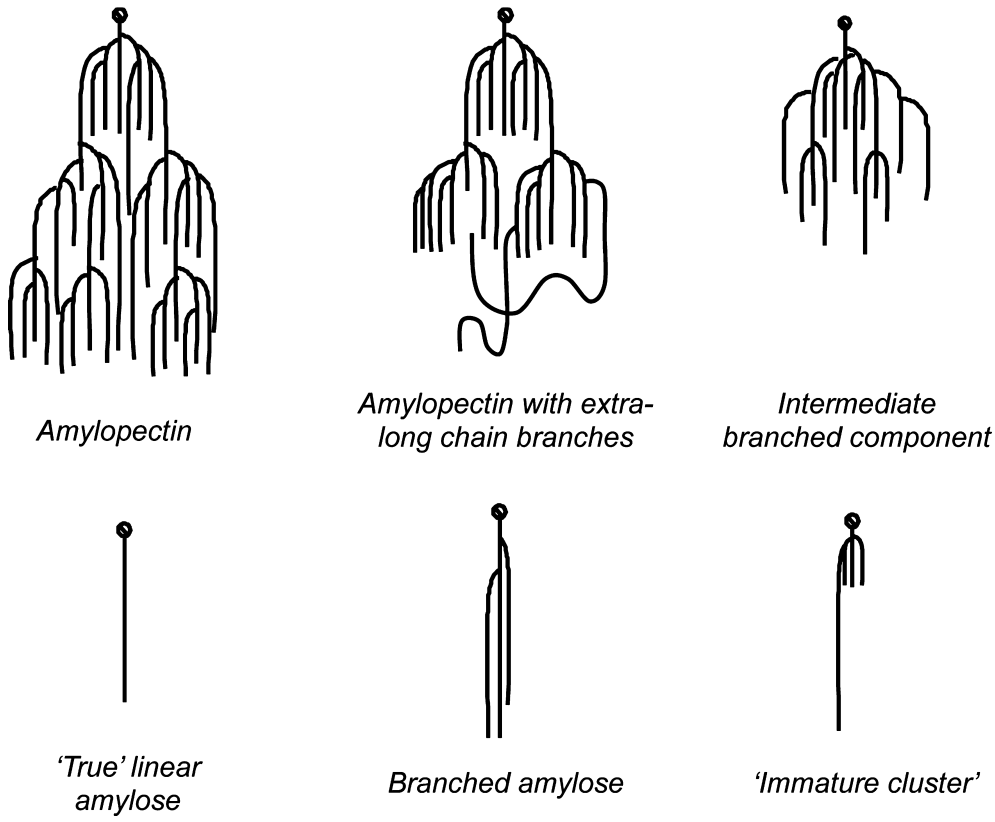

Fig. 8. Macromolecular populations found in normal (NMS) and high-amylose maize starches (G50 and G80).

an SBE cleaves an AM molecule and transfers the cleaved molecule to AP as a new branch, but this biosynthetic phenomenon has not been yet verified experimentally.

3.5.3. "True" linear and branched amylose

The existence of branched macromolecular populations in AM–apart from the linear α-glucan chains, traditionally named as "true AM"–has been documented for many decades. Pioneering work by Takeda and Hizukuri (1987), Takeda, Hizukuri, and Juliano (1989) and Takeda, Maruta, and Hizukuri (1992) identified and quantified the molar ratios, the number of branches, and the chain-length distributions of branched AM macromolecules, which are dependent on the botanical sources of the starches. The chain-length range of AM branches is broad, ranging from maltohexaose ($X_{de} = 6$) to $X_{de} \sim 20{,}000$. In the chain-length distributions of debranched AM size fractions from each starch (NMS-AM, G50-AM, and G80-AM), the size fractions with larger macromolecular sizes have longer branches, and the chain length progressively decreases with decreasing macromolecular sizes. It seems that the larger macromolecular size of AM is due to longer AM branches than larger number of branches. However, the results from the present study cannot determine the ratio of the linear and branched AM macromolecular populations in each size fraction, as they are present throughout the range of macromolecular sizes and up to this point there is no available chromatographic technology able to unambiguously separate the linear and branched AM populations. In this direction, chromatographic modes such as molecular-topology fractionation (MTF) (Edam, Meunier, Mes, Van Damme, & Schoenmakers, 2008) or temperature-gradient interaction chromatography (TGIC) (Lee, Chang, Harville, & Mays, 1998) have been reported to separate branched polystyrenes based on their degree of branching, but major technological developments are needed to implement these techniques on starch.

3.5.4. Immature clusters

Short AP-like branches are observed in every size fraction from the AM samples obtained by *n*-butanol precipitation from all starches, suggesting that besides the possibilities of AP and IC traces in the AM size fractions, there might be AM molecules with short branches. The presence of a macromolecular population resembling the architecture of an immature AP cluster that has been elongated by GBSS (Fig. 8) has been previously reported (Takeda et al., 1990). Another possibility is that these are immature AM branches that have not been elongated properly to mature long branches.

3.5.5. Intermediate component

The presence of IC in normal starches (Klucinec & Thompson, 1998; Perez & Bertoft, 2010; Vilaplana & Gilbert, 2010b) and in greater abundance in mutant starches, such as HAMS or *ae* maize mutants (Kasemsuwan et al., 1995; Wang, White, Pollak, & Jane, 1993) has been well documented in the literature. The results from the present study (Figs. 4–7 and Tables 2 and 3) reveal the differences in the branching structures between AP and IC in addition to the difference in their macromolecular sizes. The AP2/AP1 value of AP remains constant regardless of macromolecular sizes. However, the AP2/AP1 value (or the proportion of AP2 branches) in IC increases with decreasing branched macromolecular size. The higher amount of AP2 branches in HAMS compared with NMS might be due to the higher proportion of IC rather than the structure of AP in HAMS. IC also appears to have a slightly higher average DP of AP2 branches than AP, although the average DP of AP1 branches is similar between the two populations. This is consistent with that reported previously (Li et al., 2008). It seems that the chain-length distribution of AP branches is important for the crystalline structure of starch for the survival of the grain, and that the AP2/AP1 of AP is tightly controlled by starch biosynthetic enzyme machinery.

On the other hand, it seems that the altered activity of SBE in HAMS prevents IC maturing into AP and results in an abnormal structure that is less controlled by biosynthetic enzymes and that may not be involved in crystalline structure, as *ae* mutant starches have a lower degree of crystallinity than NMS (Cheetham & Tao, 1998; Matveev et al., 2001).

HAMS or *ae* mutant maize starches contain larger amounts of resistant starch (RS). The architecture of the RS residues after in vitro enzyme digestion has been assigned to two populations by Jiang et al. (2010) and Li et al. (2008): a larger population with degree of polymerisation (DP) $X \sim 1000$ and few branches that seems to originate from AM, and a smaller population of almost-linear chains with DP $X \sim 60$ that seems to originate from undigested IC. Our findings indicate that the reported higher amount of RS in HAMS can be indeed partially linked to the unique branching structure of IC, beside the large amount of AM. Upon enzyme digestion, the longer branches of IC compared to those of AP are more likely to form double helices and closely packed crystalline structures that cannot be easily accessed by enzymes, thus generating larger amounts of RS.

4. Conclusions

The two-dimensional (2D) macromolecular distributions for high-amylose maize starches (HAMS) obtained here reveal expected structural features. These include both the higher amylose (AM) content and the marked presence of intermediate component (IC), which is a macromolecular population with similar hydrodynamic size to AM but with similar chain length to amylopectin (AP), albeit having a higher ratio of lamellae-spanning branches with slightly longer chain-length. Hence there are substantial differences not only in the macromolecular sizes, but also in the branching structure between AP and IC. Tight biosynthetic control preserves the chain-length distribution of AP and the ratio of single-lamella to lamellae-spanning branches, which is fundamental for the crystalline structure of starch granules. However, amylose-extender (*ae*) mutants have a larger proportion of IC with longer lamellae-spanning branches and with a varying ratio of single-lamella and lamellae-spanning branches. This variable branching structure of IC could arise from the altered branching activities of SBE in HAMS, which may hinder the crystalline arrangement of the IC branches and prevent the IC molecules to mature into full-sized AP molecules. The presence of short AP-like branches was also confirmed in the AM fractions, suggesting the presence of immature clusters, such as immature AP that is "accidentally" elongated by granule-bound starch synthases (GBSS) and/or AM molecules with short branches that have not been elongated to mature long branches. These conclusions are made possible because the 2D method reveals features that are often masked in 1D distributions.

Acknowledgments

FV greatly appreciates the support of a postdoctoral fellowship from the Knut and Alice Wallenberg Foundation (Sweden). RGG gratefully acknowledges support from an Australian Research Council grant DP130102461.

Appendix A. Supplementary data

Supplementary data associated with this article can be found, in the online version, at http://dx.doi.org/10.1016/j.carbpol.2014.07.050.

References

Baba, T., & Arai, Y. (1984). Structural features of amylomaize starch. 3. Structural characterization of amylopectin and intermediate material in amylomaize starch granules. *Agricultural and Biological Chemistry*, *48*(7), 1763–1775.

Cave, R. A., Seabrook, S. A., Gidley, M. J., & Gilbert, R. G. (2009). Characterization of starch by size-exclusion chromatography: The limitations imposed by shear scission. *Biomacromolecules*, *10*(8), 2245–2253.

Cheetham, N. W. H., & Tao, L. (1998). Variation in crystalline type with amylose content in maize starch granules: An X-ray powder diffraction study. *Carbohydrate Polymers*, *36*(4), 277–284.

Edam, R., Meunier, D. M., Mes, E. P. C., Van Damme, F. A., & Schoenmakers, P. J. (2008). Branched-polymer separations using comprehensive two-dimensional molecular-topology fractionation × size-exclusion chromatography. *Journal of Chromatography A*, *1201*(2), 208–214.

Englyst, H. N., Kingman, S. M., & Cummings, J. H. (1992). Classification and measurement of nutritionally important starch fractions. *European Journal of Clinical Nutrition.*, *46*(Suppl 2), S33–S50.

Gaborieau, M., Gilbert, R. G., Gray-Weale, A., Hernandez, J. M., & Castignolles, P. (2007). Theory of multiple detection size exclusion chromatography of complex branched polymers. *Macromolecular Theory and Simulations*, *16*(1), 13–28.

Hanashiro, I., Itoh, K., Kuratomi, Y., Yamazaki, M., Igarashi, T., Matsugasako, J.-i., & Takeda, Y. (2008). Granule-bound starch synthase I is responsible for biosynthesis of extra-long unit chains of amylopectin in rice. *Plant and Cell Physiology*, *49*(6), 925–933.

Hanashiro, I., Matsugasako, J.-i., Egashira, T., & Takeda, Y. (2005). Structural characterization of long unit-chains of amylopectin. *Journal of Applied Glycoscience*, *52*(3), 233–237.

Hasjim, J., Cesbron-Lavau, G., Gidley, M. J., & Gilbert, R. G. (2010). In vivo and in vitro starch digestion: Are current in vitro techniques adequate? *Biomacromolecules*, *11*(12), 3600–3608.

Htoon, A., Shrestha, A. K., Flanagan, B. M., Lopez-Rubio, A., Bird, A. R., Gilbert, E. P., & Gidley, M. J. (2009). Effects of processing high amylose maize starches under controlled conditions on structural organization and amylase digestibility. *Carbohydrate Polymers*, *75*(2), 236–245.

Jane, J., Chen, Y. Y., Lee, L. F., McPherson, A. E., Wong, K. S., Radosavljevic, M., & Kasemsuwan, T. (1999). Effects of amylopectin branch chain length and amylose content on the gelatinization and pasting properties of starch. *Cereal Chemistry*, *76*(5), 629–637.

Jiang, H., Campbell, M., Blanco, M., & Jane, J.-L. (2010). Characterization of maize amylose-extender (*ae*) mutant starches: Part II. Structures and properties of starch residues remaining after enzymatic hydrolysis at boiling-water temperature. *Carbohydrate Polymers*, *80*(1), 1–12.

Kasemsuwan, T., Jane, J., Schnable, P., Stinard, P., & Robertson, D. (1995). Characterization of the dominant mutant amylose-extender (*Ae1-5180*) maize starch. *Cereal Chemistry*, *72*(5), 457–464.

Klucinec, J. D., & Thompson, D. B. (1998). Fractionation of high-amylose maize starches by differential alcohol precipitation and chromatography of the fractions. *Cereal Chemistry*, *75*(6), 887–896.

Lansky, S., Kooi, M., & Schoch, T. J. (1949). Properties of the fractions and linear subfractions from various starches. *Journal of the American Chemical Society*, *71*, 4066–4075.

Lee, H. C., Chang, T., Harville, S., & Mays, J. W. (1998). Characterization of linear and star polystyrene by temperature-gradient interaction chromatography with a light-scattering detector. *Macromolecules*, *31*(3), 690–694.

Li, L., Jiang, H., Campbell, M., Blanco, M., & Jane, J.-l. (2008). Characterization of maize amylose-extender (*ae*) mutant starches. Part I: Relationship between resistant starch contents and molecular structures. *Carbohydrate Polymers*, *74*, 396–404.

Lopez-Rubio, A., Flanagan, B. M., Shrestha, A. K., Gidley, M. J., & Gilbert, E. P. (2008). Molecular rearrangement of starch during in vitro digestion: Toward a better understanding of enzyme resistant starch formation in processed starches. *Biomacromolecules*, *9*(7), 1951–1958.

Matveev, Y. I., van Soest, J. J. G., Nieman, C., Wasserman, L. A., Protserov, V., Ezernitskaja, M., & Yuryev, V. P. (2001). The relationship between thermodynamic and structural properties of low and high amylose maize starches. *Carbohydrate Polymers*, *44*(2), 151–160.

Perez, S., & Bertoft, E. (2010). The molecular structures of starch components and their contribution to the architecture of starch granules: A comprehensive review. *Starch-Starke*, *62*(8), 389–420.

Schoch, T. J. (1942). Fractionation of starch by selective precipitation with butanol. *Journal of the American Chemical Society*, *64*(12), 2957–2961.

Takeda, Y., & Hizukuri, S. (1987). Structures of rice amylopectins with low and high affinities for iodine. *Carbohydrate Research*, *168*, 79–88.

Takeda, Y., Hizukuri, S., & Juliano, B. O. (1989). Structures and amounts of branched molecules in rice amyloses. *Carbohydrate Research*, *186*(1), 163–166.

Takeda, Y., Maruta, N., & Hizukuri, S. (1992). Examining the structure of amylose by tritium labelling of the reducing terminal. *Carbohydrate Research*, *227*, 113–120.

Takeda, Y., Shitaozono, T., & Hizukuri, S. (1990). Structures of sub-fractions of corn amylose. *Carbohydrate Research*, *199*, 207–214.

Vilaplana, F., & Gilbert, R. G. (2010a). Characterization of branched polysaccharides using multiple-detection size separation techniques. *Journal of Separation Science*, *33*(22), 3537–3554.

Vilaplana, F., & Gilbert, R. G. (2010b). Two-dimensional size/branch length distributions of a branched polymer. *Macromolecules*, *43*(17), 7321–7329.

Vilaplana, F., & Gilbert, R. G. (2011). Analytical methodology for multidimensional size/branch-length distributions for branched glucose polymers using off-line

2-dimensional size-exclusion chromatography and enzymatic treatmentJT Journal of Chromatography A. *1218*(28), 4434–4444.
Vilaplana, F., Hasjim, J., & Gilbert, R. G. (2012). Amylose content in starches: Towards optimal definition and validating experimental methods. *Carbohydrate Polymers*, *88*(1), 103–111.
Wang, Y. J., White, P., Pollak, L., & Jane, J. (1993). Characterization of starch structures of 17 maize endosperm mutant genotypes with Oh43 inbred line background. *Cereal Chemistry*, *70*, 171–179.
Whistler, R. L., & Doane, W. M. (1961). Characterization of intermediary fractions of high-amylose corn starches. *Cereal Chemistry*, *38*, 251–255.
Wu, A. C., & Gilbert, R. G. (2010). Molecular weight distributions of starch branches reveal genetic constraints on biosynthesis. *Biomacromolecules*, *11*(12), 3539–3547.
Wu, A. C., Morell, M. K., & Gilbert, R. G. (2013). A parameterized model of amylopectin synthesis provides key insights into the synthesis of granular starch. *PLoS One*, *8*(6), e65768.
Wu, A. C., Ral, J.-P., Morell, M. K., & Gilbert, R. G. (2014). New perspectives on the role of alpha-and beta-amylases in transient starch synthesis. *PLoS One*, *9*(6), e100498.